Contribution from the Department of Chemistry,
University of Iowa, Iowa City, Iowa 52242

# Reactions of $[(\eta^6\text{-}C_6(CH_3)_6)Mn(CO)_2(\eta^1\text{-}SCHSCPh_3)]BF_4$: Fast Atom Bombardment Tandem Mass Spectrometry of Dithioformate and Thioformamide Complexes. Crystal Structure of $[(\eta^6\text{-}C_6(CH_3)_6)Mn(CO)_2SCHNEt_2]^+BF_4^-$

Jeffrey L. Moler, Darrell P. Eyman,* and Larry M. Mallis[1]

*Received October 4, 1991*

The reaction of $(\eta^6\text{-}C_6(CH_3)_6)Mn(CO)_2SC(S)H$ (**1**) with $Ph_3C^+BF_4^-$ affords the adduct $[(\eta^6\text{-}C_6(CH_3)_6)Mn(CO)_2SCHSCPh_3]^+BF_4^-$ (**2**). Subsequent reaction of **2** with the nucleophiles diethylamine ($HNEt_2$), aniline ($H_2NPh$), and *tert*-butylamine ($H_2N$-*t*-Bu) produces $[(\eta^6\text{-}C_6(CH_3)_6)Mn(CO)_2SCHNEt_2]^+BF_4^-$ (**3**), $[(\eta^6\text{-}C_6(CH_3)_6)Mn(CO)_2SCHNHPh]^+BF_4^-$ (**4**), and $[(\eta^6\text{-}C_6(CH_3)_6)$-$Mn(CO)_2SCHNH$-*t*-$Bu]^+BF_4^-$ (**5**), respectively. The mass spectra of **1**-**5** and $[[(\eta^6\text{-}C_6(CH_3)_6)Mn(CO)_2]_2(\mu^2\text{-}\eta^2\text{-}SC(S)H)]^+$ (**6**) have been investigated using fast atom bombardment tandem mass spectrometry (FAB-MS/MS). Structural characterization and fragmentation patterns are derived from the collision-induced dissociation tandem mass spectra. The C-N single-bond cleavage within the N-substituted thioformamides is observed. Compounds **2**-**5** were also characterized by FTIR, FAB-MS, and $^1H$ and $^{13}C$ NMR spectroscopies. Compound **3** crystallizes in a triclinic unit cell, space group $P\bar{1}$, with $Z = 2$ and $\rho_{calc} = 1.39$ g/cm$^3$, with cell dimensions of $a = 8.312$ (6) Å, $b = 12.303$ (4) Å, $c = 13.325$ (6) Å, $\alpha = 61.14$ (3)°, $\beta = 74.69$ (5)°, $\gamma = 75.69$ (4)°, and $V = 1138$ (2) Å$^3$, obtained by a least-squares fit to 21 orientation reflections. $R$ values are $R_1 = 0.054$ and $R_2 = 0.088$ for 2475 reflections greater than $3\sigma$ above background, averaged from 4451 independent reflections that were used in the least-squares refinement.

## Introduction

The formation of transition metal dithioformates by the insertion of $CS_2$ into metal hydrogen bonds is well documented.[2] Among the characterized transition metal dithioformate complexes, the majority display $\eta^2$-coordination of the dithioformate ligand.[2a,b] Schenk et al. have reported the only study of chemical properties of $\eta^1$-dithioformate ligands.[2j] Thiolated ketone, ester, and amide derivatives of $M(CO)_5$ (M = Mn, Re) with $\eta^1$-coordination of the C=S moiety through the sulfur, but not formed from a dithioformate, have been reported.[3]

Recently, we reported the synthesis and some reactivities of two (arene)manganese dicarbonyl $\eta^1$-dithioformate compounds.[4] We report here the metal-mediated conversion of an $\eta^1$-dithioformate into thio-$C_1$ ligands, including thioformamides and alkanethiolates. An $\eta^1$-alkyl dithioformate ester intermediate is formed by the coordination of a Lewis acid to the uncoordinated sulfur of the $\eta^1$-dithioformate ligand. The N- and N,N-substituted thioformamides, resulting from the nucleophilic attack of amines on this $\eta^1$-alkyl dithioformate ester complex, retain the $\eta^1$-coordination through the sulfur to the metal. The reactions reported here have potentially useful synthetic applications in thio derivatization. In a similar vein, potassium dithioformate has been used to form thioformamide derivatives of proteins to better understand their chemical and physical properties.[5]

Fast atom bombardment mass spectrometry (FAB-MS) has been reported to be very useful for elucidating the composition and structure of organometallic complexes.[6] The energetic FAB process can lead to rearrangement or side reactions of the parent ion.[7] By using FAB tandem mass spectrometry (MS/MS) on these organometallic complexes, the parent ion is isolated and the spectra reveal information about its structural features in addition to its dissociation pathways.[8] The application of FAB-MS/MS to the analysis of several (arene)manganese dicarbonyl complexes with sulfur-coordinated dithioformate and dithioformamide ligands is reported here. In each case, fast atom bombardment ionization followed by collision-induced dissociation (CID) of the molecular ion of each of these complexes produces fragment ions consistent with the proposed structures for each complex reported here, including $[(\eta^6\text{-}C_6(CH_3)_6)Mn(CO)_2SCHNEt_2]^+BF_4^-$ whose crystal structure is also reported. The spectral fragmentation patterns reveal simple bond cleavage within the thioformamide ligands and between the metal and the coordinated ligands. The bare metal ion is observed.

## Experimental Section

**General Data.** Reactions and recrystallizations were performed under nitrogen using standard Schlenk or glovebox techniques.[9] Solvents were dried over suitable reagents, freshly distilled under dinitrogen, and deoxygenated prior to use.[10] Chromatographic separations were performed using untreated silica gel (60-200 mesh). Infrared spectra were obtained on a Mattson Cygnus 25 FTIR spectrometer; solution spectra were obtained using 0.5 mm potassium bromide cells, and solid-state spectra, using KBr mull and press techniques. FT-NMR spectra were recorded on a Bruker AC300 ($^1H$) or a WM360 ($^1H$, $^{13}C\{^1H\}$) spectrometer. $^1H$ and $^{13}C\{^1H\}$ NMR shifts are reported with respect to $\delta$ 0 for $Me_4Si$. All downfield chemical shifts are positive.

**Mass Spectrometry.** High-resolution accurate mass measurements were obtained using a VG ZAB-HF mass spectrometer in the FAB ionization mode. A VG Trio-3 tandem mass spectrometer was used to obtain FAB-MS/MS spectra.[11] The Mn complexes were dissolved in

(1) High Resolution Mass Spectrometry Facility, University of Iowa, Iowa City, Iowa 52242.

(2) (a) Yagupsky, M.; Wilkinson, G. *J. Chem. Soc. A* **1968**, 2813. (b) Palazzi, A.; Busetto, L.; Graziani, M. *J. Organomet. Chem.* **1971**, *30*, 273. (c) Albano, V. G.; Bellon, P. L.; Ciani, G. *J. Organomet. Chem.* **1971**, *31*, 75. (d) Einstein, F. W.; Enwall, E.; Flitcroft, N.; Leach, J. M. *J. Inorg. Nucl. Chem.* **1972**, *34*, 885. (e) Butler, I. S.; Fenster, A. E. *J. Organomet. Chem.* **1974**, *66*, 161. (f) Restivo, R. J.; Costin, A.; Ferguson, G.; Carty, A. J. *Can. J. Chem.* **1975**, *53*, 1949. (g) Albinati, A.; Musco, A.; Carturan, G.; Strukul, G. *Inorg. Chem. Acta* **1976**, *18*, 219. (h) Gattow, G.; Behrendt, W. In *Topics in Sulfur Chemistry*; Senning, A., Ed., Thieme: Stuttgart, Germany, 1977; Vol. 2. (i) Yaneff, P. V. *Coord. Chem. Rev.* **1977**, *23*, 183. (j) Schenk, W. A.; Schwietzke, T. *Organometallics* **1983**, *2*, 1905. (k) Bianchini, C.; Ghilardi, C. A.; Meli, A.; Midollini, S.; Orlandini, A. *Inorg. Chem.* **1985**, *24*, 932. (l) Schenk, W. A.; Kümmerle, D.; Schwietzke, T. *J. Organomet. Chem.* **1988**, *349*, 163.

(3) (a) De Filippo, D.; Lai, A.; Trogu, E. F.; Verani, G.; Preti, C. *J. Inorg. Nucl. Chem.* **1974**, *36*, 73. (b) Siedle, A. R. *Inorg. Nucl. Chem. Lett.* **1975**, *11*, 345. (c) Gingerich, R. G. W.; Angelici, R. J. *J. Organomet. Chem.* **1977**, *132*, 377. (d) Lindner, E.; Nagel, W. *Z. Naturforsch., B: Anorg. Chem., Org. Chem.* **1977**, *32B*, 1116. (e) Raubenheimer, H. G.; Kruger, G. J.; Lonbard, A. *Z. Naturforsch. B: Anorg. Chem., Org. Chem.* **1982**, *240*, C11.

(4) Schauer, S. J.; Eyman, D. P.; Bernhardt, R. J.; Wolff, M. A.; Mallis, L. M. *Inorg. Chem.* **1991**, *30*, 570.

(5) Micheel, F.; Istel, E.; Schnacke, E. *Chem. Ber.* **1949**, *82*, 131.

(6) (a) Miller, J. M. *Mass. Spectrom. Rev.* **1989**, *9*, 319. (b) Bruce, M. I.; Liddell, M. J. *J. Organomet. Chem.* **1987**, *1*, 191. (c) Liang, X.; Suwanrupha, S.; Freas, R. B. *Inorg. Chem.* **1991**, *30*, 652. (d) Bojesen, G. *Org. Mass Spectrom.* **1985**, *20*, 413.

(7) Kurlansik, L.; Williams, T. J.; Campana, J. E.; Green, B. N.; Anderson, L. W.; Strong, J. M. *Biochem. Biophys. Res. Commun.* **1983**, *111*, 478.

(8) (a) *Collision Spectroscopy*; Cooks, R. G., Ed.; Plenum: New York, 1978. (b) *Tandem Mass Spectrometry*; McLafferty, F. W., Ed.; John Wiley and Sons: New York, 1983.

(9) Shriver, D. F.; Drezdon, M. A. *The Manipulation of Air Sensitive Compounds*; Wiley: New York, 1986.

(10) Perrin, D. D.; Armarego, W. L. F. *Purification of Laboratory Chemicals*, 3rd ed.; Pergamon Press: Oxford, 1988.

0020-1669/92/1331-1816$03.00/0 

neat 3-nitrobenzyl alcohol (NBA) and placed on a standard stainless-steel FAB probe tip. The VG ZAB-HF ion source was the standard VG Analytical, Inc., design using a saddle field fast atom gun. In either case, samples were sputtered using an ~8-keV beam of xenon atoms with neutral beam currents equivalent to 2.0 mA supplied by an ION TECH (Model B 50) current and voltage regulator/meter. The molecular ions generated are mass selected by the first quadrupole mass analyzer, collisionally activated in the hexapole collision cell using Xe gas with a collision energy of 7 eV. Collision gas was introduced until the analyzer gas pressure was $7.5 \times 10^{-6}$ Torr (normal pressure: $7.5 \times 10^{-8}$ Torr). The product fragment ions formed were then mass analyzed in the second quadrupole mass analyzer. Signal adding of eight scans (3 s per scan) was performed using the multichannel analysis (MCA) software of the VG II 250 J data system.

**Materials.** (Hexamethylbenzene)manganese dicarbonyl dithioformate (**1**) was prepared by published procedures.[4] Triphenylcarbenium tetrafluoroborate ($Ph_3C^+BF_4^-$), diethylamine ($HNEt_2$), and *tert*-butylamine ($H_2N$-*t*-Bu) were purchased from Aldrich Chemical Co. and used without further purification. Aniline ($H_2NPh$), obtained from Matheson Coleman and Bell, was distilled under dinitrogen immediately prior to use.

**Syntheses. ($\eta^6$-Hexamethylbenzene)manganese Dicarbonyl Triphenylmethyl Dithioformate Tetrafluoroborate (2).** Compound **1** (200 mg, 571 μmol) and $Ph_3C^+BF_4^-$ (190 mg, 576 μmol) in THF (125 mL) were stirred for 30 min, during which the solution turned from orange to deep red. Compound **2** was not isolated from solution. $^1H$ NMR ($(CD_3)_2CO$): δ 2.39 (s, 18 H, $CH_3$) δ 7.34 (m, 15 H, CH), δ 10.75 (s, 1 H, $S_2CH$). IR (THF): $\nu_{CO}$ 1982, 1940 $cm^{-1}$. See Table III for tandem mass spectral data. $MnS_2O_2C_{34}H_{34}$: $MW_{calc}$ 593.1381; $M^+_{exp}$ *m/z* 593.1377 (Δ*m* = +0.4 mmu).

**($\eta^6$-Hexamethylbenzene)manganese Dicarbonyl *N*,*N*-Diethylthioformamide Tetrafluoroborate (3).** $HNEt_2$ (0.2 mL, 2460 μmol) was added to 125 mL of 4.57 mM (THF) solution of **2**, resulting in an immediate color change of the solution from deep red to orange. The solution was adsorbed onto silica gel and chromatographed using a hexane wash (250 mL), 5/95 acetone/hexane (200 mL), 20/80 acetone/hexane (200 mL), and 60/40 acetone/hexane (200 mL). Recrystallization of the final fraction product yielded 90 mg (40% yield) of **3** as clear orange diffractable crystals. The other fractions consisted mainly of starting material. $^1H$ NMR ($(CD_3)_2CO$): δ 1.32 (t, 6 H, $CH_3$), δ 2.35 (s, 18 H, $CH_3$), δ 3.94 (d-q, 4 H, $CH_2$), δ 8.89 (s, 1 H, SCHN). $^{13}C\{^1H\}$ NMR ($(CD_3)_2CO$): δ 227.6 (CO), δ 188.3 (SCN), δ 108.6 (ring C), δ 53.5, 48.2 ($NCH_2$), δ 16.3 (ring $CH_3$), δ 14.2, 10.9 ($NCH_2CH_3$). IR (THF): $\nu_{CO}$ 1975, 1932 $cm^{-1}$, $\nu_{CN}$ 1551 $cm^{-1}$. IR (KBr): $\nu_{CO}$ 1973, 1923 $cm^{-1}$, $\nu_{CN}$ 1552 $cm^{-1}$, $\nu_{CS}$ 1387, 1039, 596 $cm^{-1}$. See Table IV for tandem mass spectral data. $MnSO_2NC_{19}H_{29}$: $MW_{calc}$ 390.1299; $M^+_{exp}$ *m/z* 390.1284 (Δ*m* = +1.5 mmu).

**($\eta^6$-Hexamethylbenzene)manganese Dicarbonyl *N*-Phenylthioformamide Tetrafluoroborate (4).** Aniline (0.04 mL, 439 μmol) was added in 0.5 mL of THF to 125 mL of a 2.28 mM (THF) solution of **2**, resulting in a rapid color change of the solution from deep red to red-orange. The product was isolated as in **3**. The product, **4**, was obtained from the last fraction, and when dried, it yielded 33 mg (28% yield) of medium orange compound. The other fractions consisted mainly of starting material. $^1H$ NMR ($(CD_3)_2CO$): δ 2.35 (s, 18 H, $CH_3$), δ 7.40 (m, 5 H, $CH_3$), δ 9.36 (s, 1 H, NH), δ 10.71 (s, 1 H, SCHN). $^{13}C\{^1H\}$ NMR ($(CD_3)_2CO$): δ 232.6 (SCN), δ 227.1, 226.8 (CO), δ 131.8 (phenyl C), δ 108.7 (ring C), δ 16.3 (ring $CH_3$). IR (THF): $\nu_{CO}$ 1978, 1927 $cm^{-1}$, $\nu_{CN}$ 1581 $cm^{-1}$. IR (KBr): $\nu_{CO}$ 1969, 1919 $cm^{-1}$, $\nu_{CN}$ 1556 $cm^{-1}$, $\nu_{CS}$ 1385, 1038, 595 $cm^{-1}$. See Table V for tandem mass spectral data. $MnSO_2NC_{21}H_{25}$: $MW_{calc}$ 410.0986; $M^+_{exp}$ *m/z* 410.1006 (Δ*m* = −2.0 mmu).

**($\eta^6$-Hexamethylbenzene)manganese Dicarbonyl *N*-*tert*-Butylthioformamide Tetrafluoroborate (5).** *tert*-Butylamine (0.5 mL, 4760 μmol) was added in 0.5 mL of THF to 125 mL of a 3.63 mM (THF) solution of **2**, resulting in a rapid color change of the solution from deep red to orange. The product was isolated as in **3**. The product, **5**, was obtained from the second fraction, and when dried, it yielded 127 mg (72% yield) of bright orange compound. The other fractions consisted mainly of starting material. $^1H$ NMR ($(CD_3)_2CO$): δ 1.45 (s, 3 H, $NCCH_3$), δ 1.51 (s, 6 H, $NCCH_3$), δ 2.33 (s, 18 H, $CH_3$), δ 8.73, 8.75/8.84, 8.80 (d, 1 H, NH, 1:3), δ 10.18/10.90 (s, 1 H, SCHN, 1:3). $^{13}C\{^1H\}$ NMR ($(CD_3)_2CO$): δ 227.7 (CO), δ 190.6, 188.4 (SCN), δ 108.8, 108.5 (ring C), δ 62.8, 59.9, 57.7 ($NC(CH_3)_3$, δ 27.0, 26.9, 26.5 ($NC(CH_3)_3$, δ 16.3 (ring $CH_3$). IR (THF): $\nu_{CO}$ 1973, 1925 $cm^{-1}$, $\nu_{CN}$ 1581 $cm^{-1}$. IR (KBr): $\nu_{CO}$ 1967, 1916 $cm^{-1}$, $\nu_{CN}$ 1577 $cm^{-1}$, $\nu_{CS}$ 1391, 1040, 598 $cm^{-1}$. See Table VI for tandem mass spectral data. $MnSO_2NC_{21}H_{25}$: $MW_{calc}$ 390.1299; $M^+_{exp}$ *m/z* 390.1304 (Δ*m* = −0.5 mmu).

**($\eta^6$-Hexamethylbenzene)manganese Dicarbonyl *N*-Triphenylmethyl Isocyanide Tetrafluoroborate (7).** $(\eta^6\text{-}C_6(CH_3)_6)Mn(CO)_2CN$ (24 mg, 80 μmol) and $Ph_3C^+BF_4^-$ (26 mg, 79 μmol) in THF (125 mL) were stirred for 30 min, during which the solution turned from yellow to chartreuse. The yellow product, **7**, was obtained by reducing the solvent volume and adding hexane. $^1H$ NMR ($(CD_3)_2CO$): δ 2.10 (s, 18 H, $CH_3$), δ 7.30 (m, 15 H, CH). IR (THF): $\nu_{CO}$ 1998, 1956 $cm^{-1}$, $\nu_{CN}$ 2139 $cm^{-1}$.

**Table I.** Crystallographic Data for $[(\eta^6\text{-}C_6(CH_3)_6)Mn(CO)_2SCHNEt_2]^+BF_4^-$[a]

| | | | |
|---|---|---|---|
| fw | 477.25 | space group | $P\bar{1}$ (No. 2) |
| *a*, Å | 8.312 (6) | *T*, °C | 22 |
| *b*, Å | 12.303 (4) | λ, Å | 0.71073 |
| *c*, Å | 13.325 (6) | $\rho_{calc}$, g $cm^{-3}$ | 1.39 |
| α, deg | 61.14 (3) | linear abs coeff, $cm^{-1}$ | 6.9 |
| β, deg | 74.69 (5) | transm coeff | 1.00–0.97 |
| γ, deg | 75.69 (4) | $R_1$[b] | 0.054 |
| *V*, Å$^3$ | 1138 (2) | $R_2$[c] | 0.088 |
| *Z* | 2 | | |

[a] In this and subsequent tables esd's are given in parentheses. [b] $R_1 = \sum||F_o| - |F_c||/\sum|F_o|$. [c] $R_2 = [\sum w(|F_o| - |F_c|)^2/\sum w|F_o|^2]^{1/2}$, $w = 1/\sigma^2(F)$, where $\sigma^2(F) = \sigma^2(F) + (PWT \times F)^2$, PWT = 0.07.

**Crystal Structure of $[(\eta^6\text{-}C_6(CH_3)_6)Mn(CO)_2SCHNEt_2]^+BF_4^-$ (3). Collection and Reduction of X-ray Data.** Crystals of **3** were obtained as orange prisms from THF solution, upon slow addition of hexane, under dinitrogen. A crystal, 0.69 × 0.13 × 0.19 mm, sealed in a glass capillary tube with a small amount of mother liquor to prevent solvent loss, was mounted on the diffractometer. Graphite-monochromated Mo Kα radiation, average wavelength = 0.71073 Å, was used to collect data at 295 K on an Enraf-Nonius CAD4 diffractometer, using an ω scan range, 0.80 + 0.35 tan θ, and background at 25% below and above range; the horizontal aperture was varied from 2.5 to 3.0 mm depending on the angle; the scan speed ranged from 0.71 to 3.3 deg/min for a hemisphere with θ ranging from 1 to 25°. Lorentz, polarization, and empirical absorption corrections were made (μ = 6.9 $cm^{-1}$; maximum and minimum corrections, 0.97–1.0 on *F*). Three standards were used to monitor crystal decay and indicated a maximum decline in *F* of 5.5%; intensity corrections for decay were made. A total of 5192 reflections were measured for the hemisphere (±*h*,±*k*,±*l*) in reciprocal space for 2θ ranging from 2 to 50°. Averaging 4451 independent reflections greater than 3σ above background gave 2475 reflections that were used in the least-squares refinement. The cell dimensions for the triclinic crystal, space group $P\bar{1}$, *a* = 8.312 (6) Å, *b* = 12.303 (4) Å, *c* = 13.325 (6) Å, α = 61.14 (3)°, β = 74.69 (5)°, and γ = 75.69 (4)°, were obtained by a least-squares fit to 21 orientation reflections.

The positions of the manganese and sulfur atoms were located by Patterson methods. Subsequent cycles of least-squares refinement and difference Fourier calculations were used to locate all other non-hydrogen atoms and half the hydrogen atoms. During the final stages of refinement, the remaining hydrogen atom positions were calculated by assigning C–H distances of 0.95 Å and normalizing their positions with respect to located hydrogen atoms. No solvent molecules were found. Anisotropic refinement on all non-hydrogen atoms (262 variables, including scale and extinction) gave *R* values of $R_1$ = 0.054 and $R_2$ = 0.088; the standard deviation of an observation of unit weight = 1.17; the maximum parameter shift/estimated error was less than 0.04; the maximum peak height on the electron density difference map was 0.85 $e^-/Å^3$. Weights used in refinement are $1/\sigma^2(F)$, where $\sigma^2(F) = \sigma^2(F) + [(PWT)F)]^2$, PWT = 0.07, is the estimate of the propagated error due to counting error plus the estimated error based on agreement of equivalent reflections (*F* = 0.013). The data were processed using scattering factor tables provided in the Enraf-Nonius SDP software on a MicroVax 2 computer.[12] A summary of crystallographic parameters are listed in Table I.

## Results

The transformations observed in this work are summarized in Scheme I. Results of the structural study of **3** are presented in Tables I, VIII, and IX. Finally, the FAB-MS/MS studies were undertaken whose results are presented in Tables II–VII. These will be introduced at appropriate places in the sections which follow.

(11) The VG Trio-3 mass spectrometer (VG Masslabs Ltd., Altrincham, Cheshire, U.K.) has QHQ geometry (Quadrupole mass analyzer, Hexapole collision cell, Quadrupole mass analyzer).

(12) Frenz, B. A. *Enraf-Nonius Structure Determination Package*; Enraf-Nonius: College Station, TX, 1981.

## Discussion

**General Discussion.** It is assumed that the dithioformate ligand in compound **1** is $\sigma$-bonded through the sulfur to the manganese, since $^1$H NMR and IR spectral data confirm the presence of $\eta^6$-hexamethylbenzene (HMB) and two terminal carbonyls, leaving only one coordination site available for the dithioformate. Addition of triphenylcarbenium (trityl cation) to the uncoordinated sulfur of the dithioformate apparently results in significant delocalization of electrons from the metal center through the coordinated sulfur. The resulting dithioformate ester ligand is probably $\eta^1$-coordinated through sulfur to the manganese rather than $\eta^2$-coordinated to C=S as found in *fac*-$Et_4N[W(CO)_3(dppe)(\eta^1\text{-SCHS})]$ by Schenk et al.[2j] This argument is supported by the chemical shift of the dithioformate proton, which goes from 11.44 to 10.78 upon alkylation, as opposed to the much higher field shift (5.15–5.3) observed by Schenk for the $\eta^2$-coordinated ligand.[2j] This coordination has been observed in dithio esters with other metals, where the remaining coordination sphere is occupied by strong $\pi$-acceptor ligands.[13]

**Synthesis and Characterization of 2.** $(HMB)Mn(CO)_2SC(S)H$ (**1**) reacts with triphenylcarbenium tetrafluoroborate in THF at room temperature forming a red complex, the adduct $[(HMB)Mn(CO)_2SCHSCPh_3]^+BF_4^-$ (**2**), as shown in eq 1. The $^1$H NMR

$$\underset{\mathbf{1}}{[(HMB)Mn(CO)_2SCH(S)]} \xrightarrow[(THF)]{Ph_3C^+BF_4^-} \underset{\mathbf{2}}{[(HMB)Mn(CO)_2SCHSCPh_3]^+BF_4^-} \quad (1)$$

and IR spectral data indicate that the adduct has formed. The $^1$H NMR spectrum reveals a singlet peak for the six equivalent methyl groups on the arene ring and a singlet peak at $\delta$ 10.78 for the dithioformate proton. The shift for the dithioformate proton in the ester is nearly identical with shifts typically observed for the proton in bridging ($\mu^2$–$\eta^2$) dithioformate ions.[2,4,14] The infrared spectrum of **2** shows two carbonyls, shifted to higher frequency, bound to the metal. The shift in carbonyl stretching frequencies is similar to that we previously reported for the dithioformate-bridged binuclear manganese species, $[(HMB)_2Mn_2(CO)_4S_2CH]^+BF_4^-$ (**6**).[4] A similar degree of shifting of carbonyl bands to higher frequency was observed for $(HMB)Mn(CO)_2CN$ upon addition of the Lewis acids $Ph_3C^+$ and $AlMe_3$ to form the adducts $[(HMB)Mn(CO)_2CN{\cdot}CPh_3]^+BF_4^-$ (**7**) and $(HMB)Mn(CO)_2CN{\cdot}AlMe_3$.[15]

**Reactions of 2.** The reaction of **2** with secondary and primary amines, $HNEt_2$, $H_2NPh$, and $H_2N$-*t*-Bu, produces **3**–**5**, respectively. The $^1$H and $^{13}C\{^1H\}$ NMR, IR, FAB-MS, and FAB-MS/MS spectral data for compounds **3**–**5** are consistent with structures having S-coordinated thioformamide ligands, this structure was confirmed for **3** by a crystallographic structure determination. The $^1$H NMR spectrum of each reveals a singlet peak for the six equivalent methyl groups on the arene ring suggesting the presence of HMB. The infrared spectra of **3**–**5** show two carbonyl stretches, consistent with two carbonyls attached to the metal, suggesting the thioformamide ligand is monodentate; which retains an 18-electron count on the manganese. In addition, a CN stretching frequency of 1551 $cm^{-1}$ for **3** and 1581 $cm^{-1}$ for **4** and **5**, attributable to the thioformamide, is observed in solution and solid-state IR spectra. A broad band at ~1009 $cm^{-1}$, characteristic of the B–F stretching mode, in solid-state IR spectra confirms the presence of $BF_4^-$.

A proposed mechanism for the observed conversion of coordinated dithioformate to thioformamides is shown in Scheme I. Coordination of trityl cation to the uncoordinated sulfur is followed by nucleophilic attack of the amine on the dithioformate carbon. The formation of **3** apparently is made possible by the enhanced

**Scheme I**

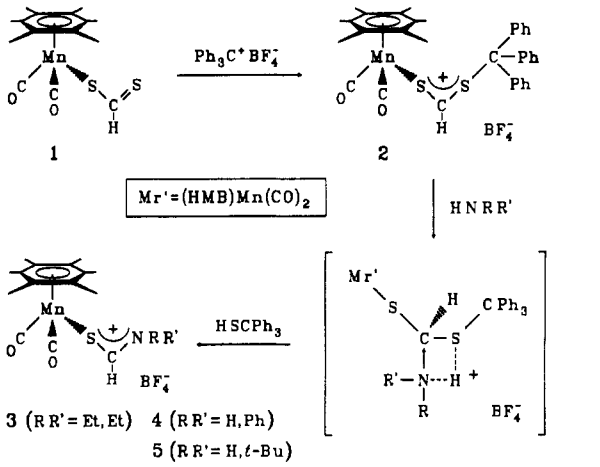


electrophilicity at the thioformyl carbon upon conversion of **1** to **2**, because we have observed that **1** does not react with excess $HNEt_2$ to give **3**. In the nucleophilic attack by an amine on the dithioformate ester cation complex, the thioformate carbon is apparently the most electrophilic site. Proton transfer from the nitrogen to the sulfur results in the formation of the coordination thioformamide and triphenylmethanethiol, similar to the acid decomposition of methyl dithio esters producing methanethiol observed by Roper et al.[16] Proton transfer from nitrogen to sulfur also has been shown to occur in the acid induced decomposition of dithiocarbamates.[17] The decomposition of the intermediate in Scheme I, an analogue of a protonated dithiocarbamate, follows the proton transfer from the amine to the alkylated sulfur. This is the reverse reaction of that observed by Miller and Latimer in their kinetic studies of dithiocarbamate decomposition, where the nitrogen protonation produced the uncoordinated amine.[18] The proposed intermediate of Scheme I is comparable to the cycloaddition product of diphenylnitrilimine with $\eta^1$-coordinated $CS_2$ shown in eq 2.[19]

$$W(CO)_3(L\text{-}L)CS_2 + PhC{\equiv}N^+\text{–}{}^-NPh \longrightarrow W(CO)(L\text{-}L)(S{=}C(SCPh)(N{=}N)Ph) \quad (2)$$

**Synthesis and Characterization of 3.** The reaction of **2** with diethylamine to produce $[(HMB)Mn(CO)_2SCHNEt_2]^+BF_4^-$ (**3**), an orange complex, is shown in eq 3. The $^1$H NMR spectrum

$$\underset{\mathbf{2}}{[(HMB)Mn(CO)_2SCHSCPh_3]^+BF_4^-} \xrightarrow[-HSCPh_3]{HNEt_2} \underset{\mathbf{3}}{[(HMB)Mn(CO)_2SCHNEt_2]^+BF_4^-} \quad (3)$$

displayed a singlet peak at $\delta$ 8.89 for the thioformyl proton. Further, the appearance of a doublet of quartets for the methylene protons of the ethyl groups suggests restricted rotation around the C–N bond, making the methylene protons of the ethyl groups nonequivalent. The methyl protons on the ethyl groups appear as a broad singlet. The $^1$H and $^{13}C\{^1H\}$ NMR spectral results are similar to those for uncoordinated *N,N*-diethylthioformamide, which shows two quartets for the methylene protons and two triplets for the methyls.[20] The presence of two resonances for

(13) (a) Schenk, W. A.; Rüb, D.; Burschka, C. *J. Organomet. Chem.* **1987**, *328*, 287. (b) *J. Organomet. Chem.* **1987**, *328*, 305.
(14) Francis, J. N.; Hawthorne, M. F. *Inorg. Chem.* **1971**, *10*, 594.
(15) $(\eta^6\text{-}C_6(CH_3)_6)Mn(CO)_2CN$, $\nu_{CO}$ = 1975, 1926 $cm^{-1}$ and $(\eta^6\text{-}C_6(CH_3)_6)Mn(CO)_2CN{\cdot}AlMe_3$, $\nu_{CO}$ = 1991, 1945 $cm^{-1}$: Weers, J. J. Ph.D. Thesis, University of Iowa, 1984.
(16) (a) Collins, T. J.; Roper, W. R.; Town, K. G. *J. Organomet. Chem.* **1976**, *121*, C41. (b) Grundy, K. R.; Harris, R. O.; Roper, W. R. *J. Organomet. Chem.* **1975**, *90*, C34.
(17) (a) Joris, S. J.; Aspila, K. I.; Chakrabarti, C. L. *J. Phys. Chem.* **1970**, *74*, 860. (b) Joris, S. J.; Aspila, K. I.; Chakrabarti, C. L. *Anal. Chem.* **1969**, *41*, 1441.
(18) Miller, D. M.; Latimer, R. A. *Can. J. Chem.* **1962**, *40*, 246.
(19) Schenk, W. A.; Kümmerle, D. *J. Organomet. Chem.* **1986**, *303*, C25.
(20) Kalinowski, H.-O.; Lubosch, W.; Seebach, D. *Chem. Ber.* **1977**, *110*, 3733.

the methylene protons implies either that rotation around the carbon–nitrogen bond is restricted due to significant C=N double bond character or that an anisotropic effect leads to methylene protons splitting each other resulting in a quartet of doublets.[21] The carbon–nitrogen bond length established by the crystal structure is 1.291 Å, shorter than the usual single, 1.472 Å, or partial double, 1.352 Å, bond lengths.[22] In fact, the carbon–nitrogen bond length is the same as that of a carbon–nitrogen double bond in a cyanodithiocarbamate ligand reported by Cotton and Harris.[23] It is therefore likely that there is sufficient double bond character to inhibit free rotation around the carbon–nitrogen bond.

**Syntheses and Characterization of 4 and 5.** The reactions of aniline and *tert*-butylamine with **2** result in the formation of $[(HMB)Mn(CO)_2SCHNHPh]^+BF_4^-$ (**4**), a dark orange complex, and $[(HMB)Mn(CO)_2SCHNH\text{-}t\text{-}Bu]^+BF_4^-$ (**5**), a light orange complex, respectively, as shown in eq 4. The unsymmetrical

$$[(HMB)Mn(CO)_2\underset{\mathbf{2}}{SCHSCPh_3}]^+BF_4^- \xrightarrow[-HSCPh_3]{HNHR} \xrightarrow[(THF)]{} [(HMB)Mn(CO)_2SCHNHR]^+BF_4^- \quad (4)$$

**4**, R = Ph
**5**, R = *t*-Bu

monosubstituted thioformamide can form cis and trans isomers due to the restricted rotation around the carbon–nitrogen bond. The $^1H$ NMR spectrum of **4** indicates that apparently only one isomer is formed with singlet peaks at $\delta$ 10.71 for the thioformyl proton and at $\delta$ 9.36 for the amide proton. The $^1H$ NMR spectral evidence for **5** indicates the formation of cis and trans isomers with singlet peaks at $\delta$ 10.18 and 10.90 for the thioformyl proton and doublets at $\delta$ 8.74 and 8.82 for the amide proton.

**Reactions of 2 with Alcohols.** The reaction of methanol and ethanol with **2** produced similar color changes in solution and a shift to lower frequency of the carbonyl stretches in the IR spectra.[24] The $^1H$ NMR spectra of the products were also consistent with *O*-alkyl thioformates, but these were not isolated. This is to be expected since coordinated *O*-alkyl thioformate ligands are reported to be unstable, dissociating even at low temperatures.[25] In our laboratories it has been observed that the product of an insertion reaction of carbonyl sulfide (COS) into a manganese hydrogen bond, presumably a thioformate, shows complete dissociation with liberation of COS at low pressure after its formation at high pressures.[26]

**Reaction of 2 with $BH_4^-$.** The addition of excess $BH_4^-$ to **2** results in a reaction which produces species that display carbonyl stretching frequencies slightly higher than those for **1**, 1972 and 1925 $cm^{-1}$, and broadened. Attempted purification by column chromatography did not effect isolation of the products. The $^1H$ NMR spectrum displays peaks for **1** and a species which we tentatively assign as an $\eta^1$-coordinated methanethiolate. The methanethiolate complex may result from hydride transfer from the product counterion, $H_3BSCPh_3^-$, to an intermediate coordinated thioformaldehyde, both possible products of $BH_4^-$ reacting with **2**. In similar reactions, the reduction of coordinated thiocarbonyls by hydride transfer has been reported to produce (thioformaldehyde)- and (methanethiolato)osmium complexes.[27]

**Table II.** Abundant Ions in the FAB Tandem Mass Spectrum of **1**

| *m/z* | structural assignment | rel abund[a] |
|---|---|---|
| 351 | $[M]^b$ | 21 |
| 295 | [M] – 2CO | 14 |
| 273 | [M] – $^-$SC(S)H and $H^+$ | 19 |
| 245 | [M] – $^-$SC(S)H, CO, and $H^+$ | 52 |
| 217 | $[Mn(HMB)]^+$ | 100 |
| 189 | [M] – HMB | 1 |
| 161 | [M] – HMB and CO | 1 |
| 133 | [M] – HMB and 2CO | 1 |
| 55 | $Mn^+$ | 1 |

[a] Abundances are relative to 100 for the most abundant analyte ion listed. [b] [M] = $[Mn(HMB)(CO)_2SC(S)H + H]^+$.

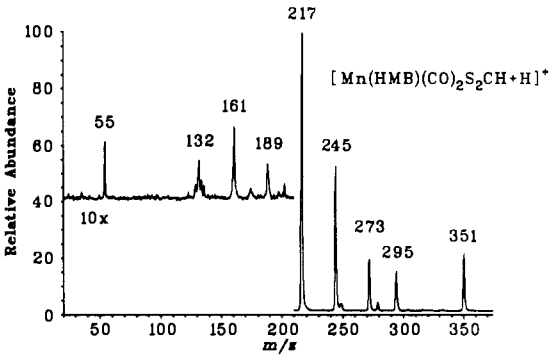


**Figure 1.** Low-energy collision spectrum of **1** (*m/z* 351).

The proposed product, $(HMB)Mn(CO)_2SCH_3$, has carbonyl stretching frequencies similar to those reported for $(\eta^6\text{-}C_6H_6)Mn(CO)_2SPh$; $\nu_{CO}$ = 1973, 1923 $cm^{-1}$.[28]

**Reaction of 2 with $BEt_3H^-$.** The addition of a stoichiometric amount of $BEt_3H^-$ to **2** results in a reaction which produces species that have carbonyl frequencies at 1969 and 1920 $cm^{-1}$. The $^1H$ NMR spectrum suggests the formation of several products including **1**, **2**, and an $\eta^1$-coordinated methanethiolate complex as was observed with $BH_4^-$. No peaks were observed that could be assigned to the proposed thioformaldehyde intermediate; however, the intermediate may have undergone rapid decomposition involving loss of thioformaldehyde.[21]

**Synthesis and Characterization of 6.** As we previously reported, the decomposition of **1** to **6** is slow under ambient conditions and increases rapidly with increasing temperature.[4] The FAB tandem MS provides an unambiguous assignment of structural features of the bridged dithioformate dimanganese complex. Similar behavior was observed for $[W(CO)_3(dppe)(SC(S)H)]^-$ decomposing to the binuclear species, $[(W(CO)_3(dppe))_2(\mu\text{-}S_2CH)]^-$ by Schenk et al.[21]

**FAB Tandem Mass Spectrometry.** Compounds **1** and **6** have previously been examined by FAB-MS and were reanalyzed by FAB tandem mass spectrometry for comparison and validation of our results.[4] In all cases, the fragment ion resulting from the loss of two carbonyls was more abundant than the fragment ion from loss of one carbonyl. This suggests that the second carbonyl is more easily dissociated than the first carbonyl alone or in conjunction with loss of part or all of the thioformamide ligand. The structural components of compounds **2–5** are unambiguously identified using FAB tandem MS. The bare metal ion (*m/z* 55) is observed in each case.

The chemical composition and relative abundance of the molecular and CID product ions of **1** (*m/z* 351) are shown in Table II; the CID FAB tandem mass spectrum of **1** is shown in Figure 1. Loss of dithioformate (*m/z* 273) and subsequent sequential loss of the two carbonyls (*m/z* 245 and 217), as well as the loss of both carbonyls (*m/z* 295) followed by loss of the dithioformate, results in the appearance of the [Mn(HMB)] (*m/z* 217) fragment ion. In addition, fragment ions showing initial loss of HMB (*m/z*

(21) (a) LaPlanche, L. A.; Rogers, M. T. *J. Am. Chem. Soc.* **1963**, *85*, 3728. (b) Siddall, T. H. (III); Stewart, W. E.; Knight, F. D. *J. Phys. Chem.* **1970**, *74*, 3580.
(22) *International Tables for X-ray Crystallography*; Kynoch Press: Birmingham, England, 1975; Vol. III, Physical and Chemical Tables.
(23) $[(C_6H_5)_4As]_2[Ni(\eta^2\text{-}S_2C{=}N{-}CN)_2]$: Cotton, F. A.; Harris, C. B. *Inorg. Chem.* **1968**, *7*, 2140.
(24) IR (THF): $[(\eta^6\text{-}C_6(CH_3)_6)Mn(CO)_2SCHOEt]^+BF_4^-$, $\nu_{CO}$ = 1979, 1931 $cm^{-1}$, and $[(\eta^6\text{-}C_6(CH_3)_6)Mn(CO)_2SCHOMe]^+BF_4^-$, $\nu_{CO}$ = 1970, 1930 $cm^{-1}$.
(25) Engler, V. R.; Gattow, G. *Z. Anorg. Allg. Chem.* **1972**, *388*, 78.
(26) Schlom, P. Ph.D. Thesis, University of Iowa, 1989.
(27) (a) Roper, W. R.; Town, K. G. *J. Chem. Soc., Chem. Commun.* **1977**, 781. (b) Collins, T. J.; Roper, W. R. *J. Organomet. Chem.* **1978**, *159*, 73. (c) Collins, T. J.; Roper, W. R. *J. Chem. Soc., Chem. Commun.* **1977**, 901.
(28) Schindehutte, M.; van Rooyen, P. H.; Lotz, S. *Organometallics* **1990**, *2*, 293.

**Table III.** Abundant Ions in the FAB Tandem Mass Spectrum of **2**

| *m/z* | structural assignment | rel abund[a] |
|---|---|---|
| 593 | [M][b] | 0.6 |
| 490 | [M] - Ph and CO | 0.2 |
| 474 | $Ph_3CSSCPh_3$ | 0.3 |
| 375 | [M] - HMB and 2CO | 0.3 |
| 351 | [M] - $Ph_3C^+$ + $H^+$ | 0.2 |
| 350 | [M] - $Ph_3C^+$ | 0.3 |
| 294 | [M] - $Ph_3C^+$ and 2CO | 0.9 |
| 273 | [M] - (S)CHSCPh$_3$ | 0.6 |
| 243 | $Ph_3C^+$ | 100 |
| 217 | $[Mn(HMB)]^+$ | 0.6 |
| 161 | [M] - HMB, CO, $Ph_3C^+$ + $H^+$ | 0.2 |
| 131 | [M] - HMB, 2CO, $Ph_3C^+$, and $H^-$ | 0.2 |
| 55 | $Mn^+$ | <0.1 |

[a] Abundances are relative to 100 for the most abundant analyte ion listed. [b] [M] = $[Mn(HMB)(CO)_2(SCHSCPh_3)]^+$.

**Table IV.** Abundant Ions in the FAB Tandem Mass Spectrum of **3**

| *m/z* | structural assignment | rel abund[a] |
|---|---|---|
| 390 | [M][b] | 6 |
| 334 | $[M]^+$ - 2CO | 100 |
| 305 | $[M]^+$ - 2CO and Et | 3 |
| 273 | $[M]^+$ - (S)CHNEt$_2$ | 2 |
| 245 | $[M]^+$ - (S)CHNEt$_2$ and CO | 5 |
| 217 | $[Mn(HMB)]^+$ | 49 |
| 172 | $[M]^+$ - HMB and 2CO | 13 |
| 55 | $Mn^+$ | 1 |

[a] Abundances are relative to 100 for the most abundant analyte ion listed. [b] [M] = $[Mn(HMB)(CO)_2SCHNEt_2]^+$.

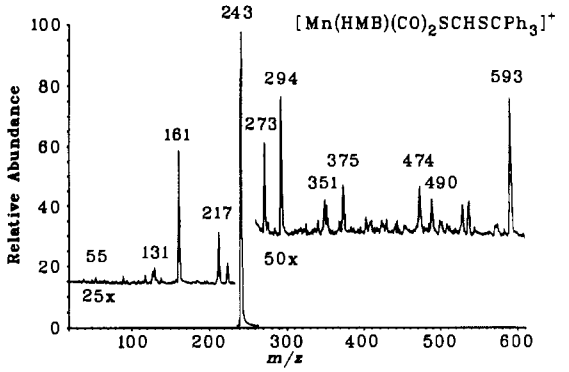


**Figure 2.** Low-energy collision spectrum of **2** (*m/z* 593).

189) followed by loss of carbonyls (*m/z* 161 and 133) are observed. These fragment ions are much lower in relative abundance due to the bonding strength of HMB to the metal. These results unambiguously characterize the structure of **1**.

The chemical composition and relative abundance of the molecular and CID product ions of **2** (*m/z* 593) are shown in Table III; the CID FAB tandem mass spectrum of **2** is shown in Figure 2. Compound **2**, formed in situ, was analyzed in a solution of tetramethylene sulfone (sulfolane). The major peak (*m/z* 243) is due to the metastable triphenylcarbenium ion. The loss of trityl cation produces $[Mn(HMB)(CO)_2(SCHS) + H^+]^+$ (*m/z* 351). The additional loss of carbonyls produces $[Mn(HMB)(SCHS) + H^+]^+$ (*m/z* 294). The loss of CO, trityl cation, and HMB results in $[Mn(CO)(SCHS) + H^+]^+$ (*m/z* 161) and $[Mn(SCS)]^+$ (*m/z* 131). $[Mn(SCHSCPh_3]^+$ (*m/z* 375) results from the loss of HMB and CO. Loss of triphenylmethyl thioformate ester and CO gives the characteristic $[Mn(HMB)]^+$ (*m/z* 217) ion. The cleavage of a C–C bond results in loss of phenyl and the loss of CO gives $[Mn(HMB)(CO)(SCHSCPh_2]^+$ (*m/z* 490). The formation of $Ph_3CSSCPh_3$ (*m/z* 375) is also observed.

The chemical composition and relative abundance of the molecular and CID product ions of **3** (*m/z* 390), **4** (*m/z* 410), and **5** (390 *m/z*) are shown in Tables IV–VI, respectively; the CID FAB tandem mass spectra of **3–5** are shown in Figures 3–5, respectively. The major product ion (*m/z* 334) for **3** and **5** is

**Table V.** Abundant Ions in the FAB Tandem Mass Spectrum of **4**

| *m/z* | structural assignment | rel abund[a] |
|---|---|---|
| 410 | [M][b] | 2 |
| 354 | [M] - 2CO | 29 |
| 319 | $[Mn(HMB)NHPh + H^+]^+$ | 8 |
| 277 | [M] - Ph and 2CO | 7 |
| 273 | [M] - (S)CHNHPh | 2 |
| 245 | [M] - (S)CHNHPh and CO | 9 |
| 217 | $[Mn(HMB)]^+$ | 100 |
| 192 | [M] - HMB and 2CO | 3 |
| 55 | $Mn^+$ | 1 |

[a] Abundances are relative to 100 for the most abundant analyte ion listed. [b] [M] = $[Mn(HMB)(CO)_2SCHNHPh]^+$.

**Table VI.** Abundant Ions in the FAB Tandem Mass Spectrum of **5**

| *m/z* | structural assignment | rel abund[a] |
|---|---|---|
| 390 | [M][b] | 7 |
| 334 | [M] - 2CO | 100 |
| 277 | [M] - *t*-Bu and 2CO | 36 |
| 273 | [M] - SCHNH-*t*-Bu | 2 |
| 245 | [M] - SCHNH-*t*-Bu and CO | 9 |
| 217 | $[Mn(HMB)]^+$ | 84 |
| 172 | [M] - HMB and 2CO | 1 |
| 55 | $Mn^+$ | <1 |

[a] Abundances are relative to 100 for the most abundant analyte ion listed. [b] [M] = $[Mn(HMB)(CO)_2SCHNH$-*t*-$Bu]^+$.

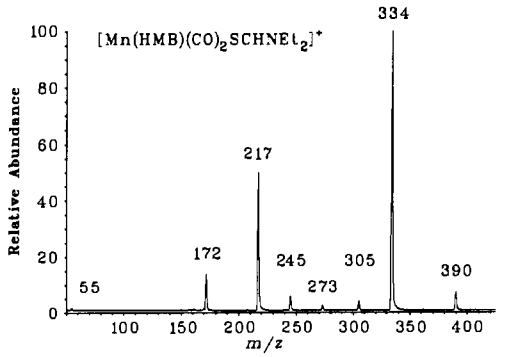


**Figure 3.** Low-energy collision spectrum of **3** (*m/z* 390).

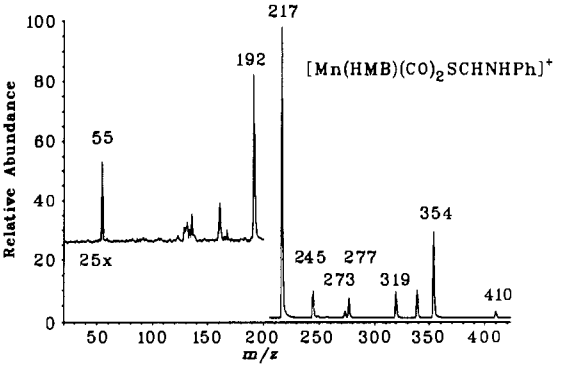


**Figure 4.** Low-energy collision spectrum of **4** (*m/z* 410).

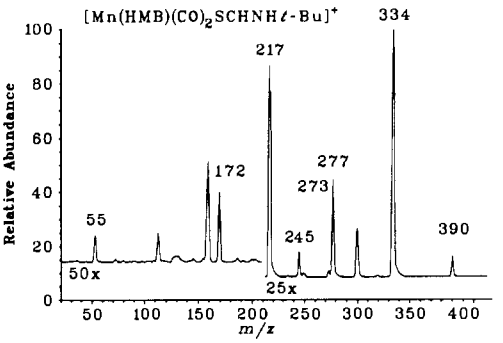


**Figure 5.** Low-energy collision spectrum of **5** (*m/z* 390).

**Table VII.** Abundant Ions in the FAB Tandem Mass Spectrum of **6**

| *m/z* | structural assignment | rel abund[a] |
|---|---|---|
| 623 | [M][b] | 40 |
| 567 | [M] - 2CO | 12 |
| 539 | [M] - 3CO | 4 |
| 511 | [M] - 4CO | 65 |
| 433 | [M] - HMB and CO | 6 |
| 405 | [M] - HMB and 2CO | 49 |
| 377 | [M] - HMB and 3CO | 14 |
| 349 | [M] - HMB and 4CO | 100 |
| 294 | [M] - Mn, HMB, and 4CO | 59 |
| 132 | [M] - Mn, 2HMB, and 4CO | 5 |
| 55 | $Mn^+$ | <2 |

[a] Abundances are relative to 100 for the most abundant analyte ion listed. [b] [M] = $[Mn_2(HMB)_2(CO)_4S_2CH]^+$.

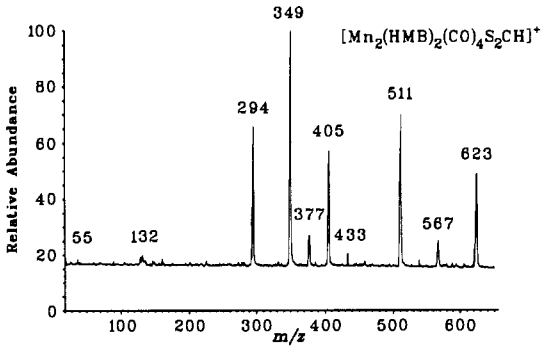


**Figure 6.** Low-energy collision spectrum of **6** (*m/z* 623).

formed by the elimination of the two carbonyl ligands. In contrast with the dissociation of **1** and **4**, which show the [Mn(HMB)] (*m/z* 217) fragment ion to be the most stable, the thioformamide ligands in **3** and **5** show stronger bonding to the metal. The HMB is more strongly bonded to Mn than are dithioformate or the thioformamides, which is indicated by the ratio of the intensities of their metal-bonded fragment ions (*m/z* 217 and 132/172/192, respectively). Consideration of the relative intensities of product ions (*m/z* 334/354/334) resulting from the loss of two carbonyls from **3**/**4**/**5**, (*m/z* 217) from $[Mn(HMB)]^+$, and (*m/z* 172/192/172) from the manganesethio formamide fragments of **3**/**4**/**5** provides an ordering of the relative strengths of the thioformamide bonding to Mn: $NEt_2$ > NH-*t*-Bu > NHPh; with respect to one another. For the monosubstituted thioformamides **4** and **5**, the bonding of the thioformamide ligand to the metal is not as enhanced as in **3**. The *tert*-butylthioformamide is more strongly bonded than the phenyl derivative. A recurring dissocation pattern is observed after the loss of the thioformamide ligand (*m/z* 273) as the two carbonyls are lost (*m/z* 245 and 217) to form the $[Mn(HMB)]^+$ fragment ion; loss of the thioformamide from *m/z* 334 in **3** and **5** and from *m/z* 354 in **4** also contributes to the intensity of this ion. The third peak (*m/z* 305) for **3** shows the cleavage of a C–N bond of one of the ethyl groups. The fourth peak (*m/z* 320) for **4** shows the cleavage of the phenyl C–N bond within the thioformamide. The third peak (*m/z* 277) for **5** shows the cleavage of the butyl C–N bond within the thioformamide. The FAB tandem mass spectral interpretation gives an unambiguous structural connectivity for **3**–**5**.

The chemical compositions and relative abundances of the molecular and CID product ions of **6** (*m/z* 623) are shown in Table VII. Within 30 s of initial bombardment, the bridged binuclear species **6** is formed from **1** in the FAB ion source. The CID FAB tandem mass spectrum of **6** is shown in Figure 6. Carbonyls are removed in pairs from the bridged dithioformate dimanganese complex: loss of the first two carbonyls results in the fragment ion at *m/z* 567 and an additional loss of another pair results in the fragment ion at *m/z* 511. All but three of the fragment ions (*m/z* 294, 132, and 55, the bare metal ion) retain the bridging dithioformate indicating an enhanced strength of the M–S bonds. The enhanced stability of the bridged species allows the scission of one HMB as evidenced by fragment ions that show loss of one carbonyl (*m/z* 433), two carbonyls (*m/z* 405), three carbonyls (*m/z* 377), and all four carbonyls (*m/z* 349), which gives the major fragment ion. The bare metal ion (*m/z* 55) is also observed. This dissociation pattern is more straightforward than the comparable FAB mass spectrum reported previously, since all observed fragments must result from the molecular ion.[4]

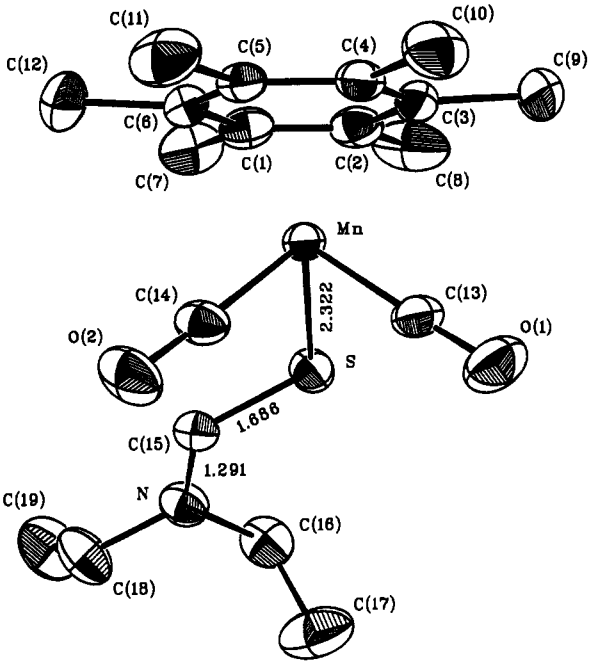


**Figure 7.** ORTEP drawing of **3** (25% probability ellipsoids).

**Table VIII.** Fractional Coordinates and Isotropic Thermal Parameters[a] for **3**

| atom | *x* | *y* | *z* | $B_{iso}$, Å$^2$ |
|---|---|---|---|---|
| Mn | 0.22583 (8) | 0.10341 (6) | 0.24722 (5) | 3.76 (1) |
| S | −0.0341 (2) | 0.2206 (1) | 0.2716 (1) | 5.15 (3) |
| C(1) | 0.3004 (7) | 0.2632 (5) | 0.0780 (4) | 5.2 (1) |
| C(2) | 0.2169 (7) | 0.1893 (5) | 0.0606 (4) | 5.7 (1) |
| C(3) | 0.2738 (6) | 0.0596 (4) | 0.0995 (4) | 5.1 (1) |
| C(4) | 0.4119 (7) | 0.0038 (4) | 0.1614 (4) | 4.7 (1) |
| C(5) | 0.4938 (6) | 0.0761 (4) | 0.1793 (3) | 4.3 (1) |
| C(6) | 0.4390 (6) | 0.2098 (4) | 0.1350 (4) | 4.7 (1) |
| C(7) | 0.243 (1) | 0.4052 (6) | 0.0316 (6) | 8.1 (2) |
| C(8) | 0.0680 (9) | 0.2515 (9) | −0.0061 (5) | 10.7 (3) |
| C(9) | 0.1922 (9) | −0.0226 (6) | 0.0778 (5) | 8.8 (2) |
| C(10) | 0.468 (1) | −0.1355 (5) | 0.2028 (5) | 7.8 (2) |
| C(11) | 0.6412 (8) | 0.0222 (7) | 0.2428 (5) | 7.9 (2) |
| C(12) | 0.5342 (9) | 0.2888 (5) | 0.1487 (6) | 8.2 (2) |
| C(13) | 0.1229 (7) | −0.0325 (4) | 0.3344 (4) | 5.1 (1) |
| O(1) | 0.0590 (6) | −0.1207 (4) | 0.3883 (4) | 8.0 (1) |
| C(14) | 0.2762 (6) | 0.0903 (5) | 0.3745 (4) | 5.2 (1) |
| O(2) | 0.3132 (5) | 0.0828 (4) | 0.4550 (3) | 7.7 (1) |
| C(15) | −0.0260 (6) | 0.3111 (4) | 0.3325 (4) | 4.6 (1) |
| N | −0.1552 (6) | 0.3786 (4) | 0.3634 (3) | 5.5 (1) |
| C(16) | −0.3263 (8) | 0.3807 (5) | 0.3501 (5) | 6.7 (2) |
| C(17) | −0.417 (1) | 0.287 (1) | 0.4534 (7) | 10.8 (3) |
| C(18) | −0.134 (1) | 0.4464 (5) | 0.4245 (5) | 7.5 (2) |
| C(19) | −0.195 (1) | 0.5852 (6) | 0.3659 (7) | 10.0 (3) |
| B | 0.2858 (9) | 0.5915 (6) | 0.2242 (5) | 6.1 (2) |
| F(1) | −0.265 (1) | 0.3752 (5) | 0.6999 (5) | 21.4 (3) |
| F(2) | 0.5519 (8) | 0.3953 (6) | −0.1653 (6) | 14.1 (3) |
| F(3) | 0.1917 (8) | 0.658 (1) | 0.1623 (7) | 27.8 (5) |
| F(4) | 0.2669 (9) | 0.4700 (5) | 0.2782 (7) | 16.9 (3) |

[a] Values for anisotropically refined atoms are given in the form of the isotropic equivalent displacement parameter defined as $(4/3)[a^2B(1,1) + b^2B(2,2) + c^2B(3,3) + ab(\cos\gamma)B(1,2) + ac(\cos\beta)B(1,3) + bc(\cos\alpha)B(2,3)]$.

**Crystallographic Study of 3.** The crystallographic study was performed to establish the molecular structure of **3**, which is illustrated in ORTEP plot in Figure 7. Positional parameters are reported in Table VIII. Selected bond distances and angles are

**Table IX.** Interatomic Bond Distances (Å) and Angles (deg) for **3**

| Distances | | | |
|---|---|---|---|
| Mn–C(1) | 2.216 (5) | C(1)–C(2) | 1.40 (1) |
| Mn–C(2) | 2.197 (6) | C(1)–C(6) | 1.394 (8) |
| Mn–C(3) | 2.198 (6) | C(1)–C(7) | 1.536 (9) |
| Mn–C(4) | 2.164 (5) | C(2)–C(3) | 1.41 (1) |
| Mn–C(5) | 2.178 (5) | C(2)–C(8) | 1.54 (1) |
| Mn–C(6) | 2.221 (6) | C(3)–C(4) | 1.426 (9) |
| Mn–C(13) | 1.783 (7) | C(3)–C(9) | 1.51 (1) |
| Mn–C(14) | 1.776 (6) | C(4)–C(5) | 1.379 (9) |
| Mn–S | 2.322 (2) | C(4)–C(10) | 1.512 (9) |
| S–C(15) | 1.686 (6) | C(5)–C(6) | 1.448 (8) |
| N–C(15) | 1.291 (8) | C(5)–C(11) | 1.504 (9) |
| N–C(16) | 1.47 (1) | C(6)–C(12) | 1.49 (1) |
| N–C(18) | 1.482 (9) | C(16)–C(17) | 1.46 (1) |
| O(1)–C(13) | 1.142 (8) | C(18)–C(19) | 1.51 (1) |
| O(2)–C(14) | 1.150 (7) | C(15)–H(19) | 0.947 (1) |
| **Angles** | | | |
| S–Mn–C(13) | 87.1 (2) | C(16)–N–C(18) | 118.5 (6) |
| S–Mn–C(14) | 91.8 (2) | N–C(16)–C(17) | 112.7 (7) |
| C(13)–Mn–C(14) | 89.5 (3) | N–C(18)–C(19) | 113.3 (7) |
| Mn–C(13)–O(1) | 178.3 (6) | C(1)–C(2)–C(3) | 120.3 (6) |
| Mn–C(14)–O(2) | 178.0 (6) | C(2)–C(3)–C(4) | 119.3 (5) |
| Mn–S–C(15) | 111.5 (2) | C(3)–C(4)–C(5) | 120.6 (5) |
| S–C(15)–N | 124.4 (5) | C(4)–C(5)–C(6) | 119.7 (5) |
| C(15)–N–C(16) | 122.0 (5) | C(5)–C(6)–C(1) | 119.5 (6) |
| C(15)–N–C(18) | 119.2 (6) | C(6)–C(1)–C(2) | 120.6 (6) |
| S–C(15)–H(19) | 117.2 (6) | N–C(15)–H(19) | 118.5 (6) |

given in Table IX. As seen in Figure 7, the molecule has a "piano stool" arrangement with the three ligands underneath in a staggered configuration with respect to the ring carbons. The HMB ring is slightly tilted away from the sulfur as evidenced by the shorter Mn–C bonds to C(4) and C(5), which are greater than the bonds to C(1) and C(2).

The bonding in the manganese thioformamide fragment of **3** is of particular interest in understanding the results of spectroscopic methods used in the characterization of **3–5**. The Mn–S bond, 2.322 Å, is shorter than that in $[(C_6H_5)_2P–CH_2–P(C_6H_5)_2]Mn(CO)_3(\eta^2\text{-}S_2CH)$ (Mn–S = 2.40 and 2.39 Å)[29] and $(\eta^6\text{-}C_6H_6)Mn(CO)_2SPh$ (Mn–S = 2.350 Å),[28] but is between the distances in $[Mn_2(CO)_6(\mu\text{-}S_2CPCy_3)]$ (Mn(I)–S bonds = 2.282, 2.276, 2.335, and 2.332 Å),[30] all suggesting a very strong Mn–S interaction. The carbon–sulfur bond length, 1.686 Å, is equal to the shorter of the two C–S bonds in $Ni[\eta^2\text{-}S_2C–NH_2]_2$,[31] $NH_4[S_2C–NH_2]$,[32] and the aforementioned cyanodithiocarbamate.[23] The carbon–nitrogen bond of the thioformamide is equal in length to the carbon–nitrogen double bond in the aforementioned cyanodithiocarbamate.[23] The atoms Mn, S, C(15), H(19) (the thioformyl hydrogen), N, C(16), and C(18) were all found to lie in the same plane by least-squares plane analysis results listed in supplemental Table SV. Bond angles within the *N,N*-diethylthioformamide ligand are S–C(15)–N = 124.4°, S–C(15)–H(19) = 117.8°, N–C(15)–H(19) = 117.8°, C(15)–N–C(16) = 122.0°, C(15)–N–C(18) = 119.2°, and C(16)–N–C(18) = 118.5°, which indicate significant $sp^2$ character in the bonding of the amide N. The planar geometry about the nitrogen indicates that the lone pair electrons have been delocalized into the N–C–S $\pi$-bonding system. This results in decreased length of the C–N bond and inequivalence of the methylene protons in the $^1H$ NMR spectrum resulting from hindered rotation about that bond.

## Conclusions

Triphenylcarbenium ion reacts with **1**, not with hydride abstraction, but by simple addition to the uncoordinated sulfur of the $\eta^1$-dithioformate. Addition of either secondary or primary amines to the $\eta^1$-coordinated alkyl dithioformate ester results in the nucleophilic displacement of the thiolate to form thioformamide complexes. Other nucleophiles, such as alcohols and hydrides, produce analogous displacement reactions forming thioformates, thioformaldehyde, and methanethiolate complexes, which are less stable than the thioformamides. Addition of other Lewis acids to the uncoordinated sulfur of **1** would probably produce similar reactivity at the thioformyl carbon. The $\eta^1$-dithioformate ester ligand donates more electron density than the *N*-alkylthioformamides; this is indicated by carbonyl stretching frequencies which decrease with increasing electron density on the metal. The FAB-MS/MS data suggest a strong Mn–S bond, which may arise because of delocalization of electron density through the Mn–S–C–N bonds. The crystal structure of **3** reveals substantial delocalization of the nitrogen lone-pair electrons through the N–C–S moiety of the ligand, resulting in planarity.

**Acknowledgment.** We wish to thank Steven J. Schauer for his initial contribution to this area of research and Norman C. Baenziger for his assistance in learning X-ray diffraction analysis. Acknowledgment is made to the Office of Research and Educational Development at the University of Iowa for partial support of this research and funds to purchase the VG ZAB-HF mass spectrometer. The Bruker WM-360 NMR and the Enraf-Nonius CAD-4 diffractometer were purchased in part with funds from the National Science Foundation (Grants CHE82-01836 and CHE85-07623, respectively).

**Supplementary Material Available:** Listings of complete crystallographic and data collection parameters (Table SI), general displacement parameter expressions (Table SII), hydrogen atom coordinates (Table SIII), additional bond lengths and angles (Table SIV), and least-squares planar analysis (Table SV) and an additional ORTEP drawing (6 pages); a table of observed and calculated structure factors (13 pages). Ordering information is given on any current masthead page.

(29) Einstein, F. W.; Enwall, E.; Flitcroft, N.; Leach, J. M. *J. Inorg. Nucl. Chem.* **1972**, *404*, 71.
(30) Miguel, D.; Riera, V. *Organometallics* **1991**, *10*, 1683.
(31) (a) Engler, R.; Kiel, G.; Gattow, G. *Z. Anorg. Allg. Chem.* **1974**, *404*, 71. (b) Gasparri, G. F.; Nardelli, M.; Villa, A. C. *Acta Crystallogr.* **1967**, *23*, 384.
(32) Capacchi, L.; Villa, A. C.; Ferrari, M.; Nardelli, M. *Ric. Sci., Parte II: Sez. A* **1967**, *37*, 993.